<Brief Note>

Optimization of protein complex formation conditions using an improved modified cell-penetrating peptide

Momoka Narita[1] and Akiko Okuda[1,*]

Summary Cell-penetrating peptides (CPPs) are widely used as intracellular delivery tools for proteins and other macromolecules; however, their low cytosolic delivery efficiency remains a major limitation. To overcome this issue, Pas2r12, an improved modified CPP, was developed. Pas2r12 forms complexes with proteins such as enhanced green fluorescent protein (EGFP) and immunoglobulin G and mediates their cytosolic delivery into cells. Pas2r12–EGFP complexes are typically prepared by simple mixing followed by static incubation; however, this method has not been optimized for delivery efficiency. We investigated the effects of vortex mixing and incubation time on cytosolic EGFP delivery in HEK293 cells. Vortex-assisted preparation with 1 hour incubation improved delivery efficiency, up to 130%, whereas other incubation conditions (0.5 h and 2 h) or preparation without vortex mixing demonstrated no improvement.

Particle analysis by confocal microscopy revealed heterogeneous sizes ranging from 0.41 to 1.44 μm, and flow cytometry indicated differences in particle distribution and internal complexity. Notably, no clear correlation was observed between particle size and delivery efficiency. The observed particle sizes exceeded those typically associated with caveolae-mediated endocytosis (~80 nm), suggesting the involvement of alternative uptake pathways. Together with our previous finding that Pas2r12–EGFP is predominantly internalized via caveolae-mediated endocytosis, these results support a model in which multiple uptake mechanisms contribute depending on particle properties.

Altogether, these findings demonstrate that mixing conditions and incubation time critically affect complex formation and delivery performance and suggest that not only particle size but also particle uniformity and structural properties are key determinants of efficient intracellular delivery.

Key words: Cell-penetrating peptide, Drug delivery system, Enhanced green fluorescent protein, Cytosolic protein delivery

1. Introduction

Intracellular delivery of proteins and peptides remains a critical challenge in drug discovery and molecular imaging. Cell-penetrating peptides (CPPs), such as HIV-1 TAT peptide[1] and oligoarginines[2], have emerged as versatile tools for the efficient translocation of high-molecular-weight compounds, such as proteins, into cells[3]. Despite

[1]Faculty of Medicine, School of Health Sciences, Niigata University, 2-746 Asahimachi-dori, Chuo-ku, Niigata 951-8518, Japan.

*Corresponding author: Akiko Okuda, Faculty of Medicine, School of Health Sciences, Niigata University, 2-746 Asahimachi-dori, Chuo-ku, Niigata 951-8518, Japan.
Tel: +81-25-227-2387
Fax: +81-25-227-2387
E-mail: okudaa.clg@niigata-u.ac.jp

Received for Publication: April 3, 2026
Accepted for Publication: May 27, 2026

their widespread applicability, the impact of complex formation conditions and physicochemical properties of CPP–cargo assemblies on delivery efficiency remains incompletely understood[4]. Heterogeneity in complex size, aggregation, and self-quenching of fluorescently labeled molecules can potentially affect experimental outcomes.

Recent research on nanoparticles has emphasized the importance of controlled mixing and particle state management to achieve uniform and stable complex formation[5]. Quantitative evaluation of particle size, number, internal structure, and fluorescence characteristics is now feasible by flow cytometry[6,7], dynamic light scattering[8], and nanoparticle tracking analysis[9], thereby enabling detailed characterization of the relationship between complex formation conditions and particle properties.

On the other hand, many CPP-mediated cargoes are trapped within endosomes after cellular uptake, resulting in limited cytosolic delivery efficiency[10]. To overcome this limitation, the penetration-accelerating sequence (Pas; FFLIPKG) was developed[11]. Pas was shown to enhance oligoarginine-mediated intracellular delivery of molecules up to approximately 15 kDa. Pas2r12, which we previously developed, consists of tandem repeats of a modified Pas sequence (FFLIG)[12] conjugated with oligoarginine residues[13]. We demonstrated that Pas2r12 forms complexes with proteins such as enhanced green fluorescent protein (EGFP) and immunoglobulin G (IgG) and delivers them into the cytosol of HEK293 cells mainly via caveolae-mediated endocytosis. In addition, our previous phosphoproteomic analysis suggested that Pas2r12–EGFP complexes activate intracellular signaling pathways including ERK1/2, implying that these complexes may induce cellular responses during uptake[14,15]. Furthermore, the insulin receptor has been suggested as one of the potential cell-surface receptors involved in the uptake of Pas2r12–EGFP complexes[16]. One of the characteristic properties of Pas2r12 is that it forms complexes with proteins through simple mixing without requiring chemical crosslinking or covalent modification. Conventionally, these complexes are prepared by simple mixing followed by incubation; however, the effects of physical mixing conditions on particle uniformity and delivery efficiency have not been systematically investigated.

Therefore, we conducted this study to explore the impact of vortex mixing and incubation time on the formation of Pas2r12–EGFP complexes and their cytosolic delivery into HEK293 cells. We compared the particle size, internal structure, fluorescence intensity, and particle number by confocal laser microscope and flow cytometry to clarify the relationship between complex formation conditions and intracellular delivery efficiency.

Our aim is to identify optimal conditions for the efficient formation of Pas2r12–EGFP complexes and effective cytosolic delivery, thereby improving our understanding of the relationship between complex formation conditions and intracellular delivery efficiency.

2. Materials and Methods

Cell line

HEK293 cells (human embryonic kidney–derived cells) were purchased from the JCRB Cell Bank (Osaka, Japan) and cultured in Dulbecco's modified Eagle medium (DMEM; Thermo Fisher Scientific, Waltham, MA, USA) supplemented with 10% fetal bovine serum (FBS; Corning, Corning, NY, USA) at 37°C in a humidified atmosphere containing 5% CO_2. The cells were passaged every 5–7 days and used for experiments.

Peptide preparation

Pas2r12 (FFLIGFFLIGrrrrrrrrrrr-amide; molecular weight: 3,046.7, where uppercase letters indicate l-amino acids and lowercase letters indicate d-amino acids) was synthesized and purified by Scrum Inc. (Tokyo, Japan). It was dissolved in ultrapure water before use.

Preparation of EGFP

All recombinant DNA experiments were conducted according to the regulations for biosafety at Niigata University under approved containment

measures for Class I use (approval number: SD2052).

EGFP with a histidine tag was overexpressed in *Escherichia coli* BL21 (DE3) cells (BioDynamics Laboratory, Tokyo, Japan) and purified from bacterial lysates using Ni-NTA agarose (Qiagen, Hilden, Netherlands)[17]. The purified EGFP was buffer-exchanged into phosphate-buffered saline and concentrated using an ultrafiltration membrane (Vivaspin 6-PES 30,000 MWCO; Sartorius, Göttingen, Germany). EGFP concentration was determined by measuring the absorbance at 488 nm.

Preparation of Pas2r12–EGFP complexes

Table 1 summarizes the preparation conditions for Samples 1–6. DMEM (Thermo Fisher Scientific, Waltham, MA, USA) was used as the solvent for complex formation. Pas2r12–EGFP complexes were prepared using two methods (Fig. 1).

In Method A, Pas2r12 and EGFP were added to serum-free DMEM to final concentrations of 20 and 15 μmol/L, respectively, and the total volume was adjusted to 100 μL. The mixture was then incubated at 24°C for 0.5, 1, or 2 h (Samples 1, 3, and 5).

In Method B, an EGFP solution (30 μmol/L, total volume 50 μL) and a Pas2r12 solution (40 μmol/L, total volume 50 μL) were prepared separately in DMEM. The Pas2r12 solution was added to the EGFP solution in 2.5-μL aliquots at 10-s intervals under vortex mixing with a TOUCH MIXER MIT-31 (Yamato Scientific Co., Ltd., Tokyo, Japan) to obtain a final mixture (total volume 100 μL) containing 15 μmol/L EGFP and 20 μmol/L Pas2r12.

Table 1 Preparation conditions for Pas2r12–EGFP samples.

Sample No	1	2	3	4	5	6
Vortex mixing	–	+	–	+	–	+
Incubation (h)	0.5	0.5	1	1	2	2

Pas2r12–EGFP complexes were prepared according to the method illustrated in Fig. 1. Sample 3 corresponds to the conventional preparation condition.

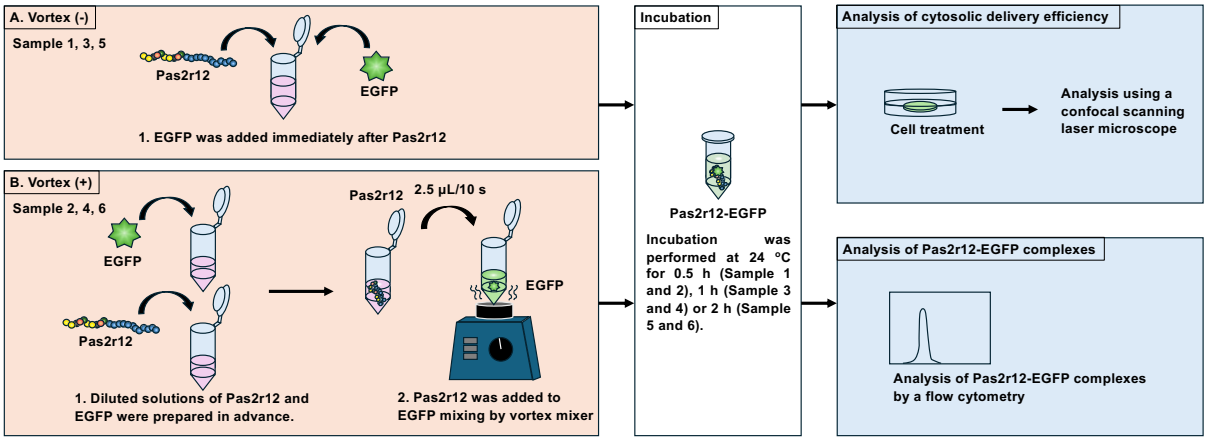

Fig. 1. Preparation and analysis of Pas2r12–EGFP complexes. The preparation conditions for Samples 1–6 are summarized in Table 1. Dulbecco's modified Eagle medium (DMEM) was used as the solvent for complex formation. Pas2r12–enhanced green fluorescent protein (EGFP) complexes were prepared using two methods. In Method A, Pas2r12 and EGFP were added to serum-free DMEM to final concentrations of 20 and 15 μmol/L, respectively, and the total volume was adjusted to 100 μL. The mixture was incubated for 0.5, 1, or 2 h (Samples 1, 3, and 5). In Method B, EGFP (30 μmol/L, 50 μL) and Pas2r12 (40 μmol/L, 50 μL) were prepared separately in DMEM. The Pas2r12 solution was added to the EGFP solution in 2.5-μL aliquots at 10-s intervals under vortex mixing to obtain a final mixture (100 μL) containing 15 μmol/L EGFP and 20 μmol/L Pas2r12. The mixture was then incubated for 0.5, 1, or 2 h, as in Method A (Samples 2, 4, and 6). Samples 1 and 2 correspond to 0.5-h incubation, Samples 3 and 4 correspond to 1-h incubation, and Samples 5 and 6 correspond to 2-h incubation.

The mixture was then incubated at 24°C using a MiniT-C Petit Cool incubator (WakenBtech Co., Ltd., Kyoto, Japan) for 0.5, 1, or 2 h, as in Method A (Samples 2, 4, and 6).

Samples 1 and 2 corresponded to 0.5 h of incubation, Samples 3 and 4 corresponded to 1 h of incubation, and Samples 5 and 6 corresponded to 2 h of incubation.

Analysis of the cytosolic delivery efficiency of EGFP mediated by Pas2r12

HEK293 cells (5×10^4 cells/mL) were seeded (2 mL) in 35-mm glass-bottom dishes (Iwaki, Tokyo, Japan) and cultured for 5 days in DMEM supplemented with 10% FBS. The medium was then replaced with DMEM containing 2.5% FBS, and the cells were further cultured overnight [18].

After removing the medium, 100 µL of the Pas2r12–EGFP complex solution prepared under each condition (Fig. 1) was added to the center of the glass-bottom dish, and the cells were incubated for 45 min at 37°C. For experiments involving filtration through a 48-µm nylon mesh, 200 µL of the Pas2r12–EGFP solution was prepared, and the entire volume was passed through the nylon mesh. Subsequently, 100 µL of the filtered solution was added to the cells.

Then, 2 mL of DMEM (supplemented with 10% FBS) and 2 µL of Hoechst 33342 (1 mg/mL; nuclear staining dye) were added, followed by incubation for 30 min at 37°C. The medium containing Hoechst 33342 was then removed, and 2 mL of fresh DMEM (10% FBS) was added.

Intracellular EGFP was observed using a confocal laser scanning microscope (FV1200 ; Olympus, Tokyo, Japan). From the obtained images, the total number of cells was determined from nuclear staining images using ImageJ[19], and the number of cells demonstrating cytosolic EGFP localization was counted by visual inspection from EGFP images. The cytosolic delivery efficiency of EGFP was calculated as the number of cells with cytosolic EGFP divided by the total number of cells per five fields of view multiplied by 100. All experiments were independently performed three times (n = 3). Statistical analyses were performed using one-way analysis of variance (ANOVA) followed by Dunnett's multiple comparison test. This study was conducted as an initial proof-of-concept study to evaluate intracellular EGFP delivery and the formation conditions of Pas2r12–EGFP complexes. Therefore, three independent experiments were performed to assess reproducibility and overall statistical trends among experimental conditions.

Analysis of Pas2r12–EGFP complex under confocal laser scanning microscope

A 6.5-µL aliquot of the Pas2r12–EGFP solution prepared as described in materials and methods of preparation of Pas2r12–EGFP complexes section was mixed with 2.5 µL of mounting medium (Dako, Glostrup, Denmark), and a coverslip was applied. Fluorescence imaging was performed at 488 nm using a confocal laser scanning microscope (FV1200) equipped with a 60× objective lens.

Particle areas were measured from images of 15 fields of view using ImageJ. The area data were then log10-transformed and used for subsequent analysis and graphing. Particle diameters were calculated from the measured particle area assuming a circular shape. The diameter (d) was determined using the following equation:

$$d = 2\sqrt{\frac{a}{\pi}}$$

Analysis of Pas2r12–EGFP complexes by flow cytometry

The Pas2r12–EGFP solution (100 µL) prepared as described in Section 4 was diluted with 300 µL of phosphate buffered saline (PBS) and passed through a 48-µm nylon mesh filter. A 200-µL aliquot of this solution was then subjected to flow cytometric analysis using NovoCyte Flow Cytometer System (Agilent Technologies, Santa Clara, CA, USA).

For data obtained from three independent experiments, the geometric mean (Geo mean) values of forward scatter (FSC), side scatter (SSC), EGFP fluorescence intensity, and particle counts were calculated, and the average values were plotted. All experiments were independently performed three

times (n = 3). Flow cytometric analysis was conducted as a comparative evaluation of particle characteristics among different preparation conditions to assess reproducibility and overall trends in particle properties. Statistical analyses were performed using one-way ANOVA followed by Dunnett's multiple comparison test using Sample 3 as the control condition.

3. Results and Discussion

Effect of vortex mixing and incubation time on cytosolic delivery efficiency

Conventionally, Pas2r12–EGFP complexes have been prepared by simply adding EGFP to a Pas2r12 solution followed by static incubation for 1 h (Table 1, Sample 3). Nevertheless, this method has not been systematically optimized with regard to complex uniformity or cytosolic delivery efficiency.

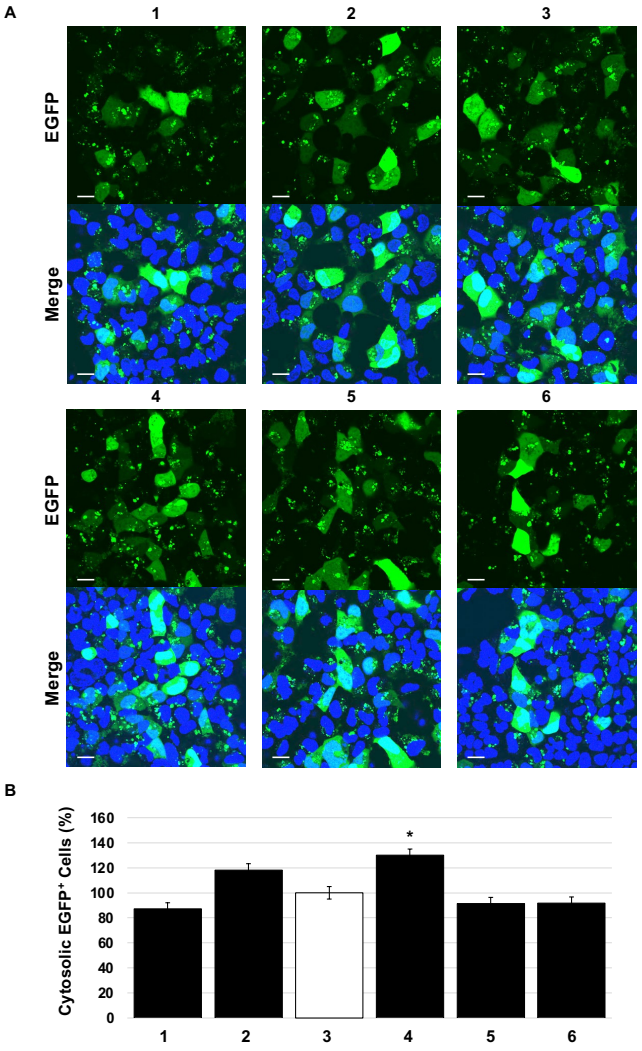

Fig. 2. Cytosolic delivery of EGFP mediated by Pas2r12. (A) Confocal laser scanning microscopy images illustrating the intracellular localization of enhanced green fluorescent protein (EGFP). Blue indicates Hoechst 33342 (nuclear staining), and green indicates EGFP. Merge represents the overlay of EGFP and Hoechst 33342 signals. Scale bar: 20 μm. (B) Quantitative analysis of cytosolic EGFP delivery depicted in (A). Delivery efficiency was compared among different conditions. Data are expressed as mean ± SD (n = 3). Sample 3 was used as the control, and statistical analysis was conducted using one-way analysis of variance (ANOVA) followed by Dunnett's multiple comparison test. $*p < 0.05$.

Therefore, in the present study, we introduced an initial vortex mixing step and varied the incubation time (0.5, 1, and 2 h) to determine their effects on cytosolic delivery efficiency in HEK293 cells (Fig. 1). Vortex-assisted preparation followed by incubation for 1 h (Sample 4) significantly improved the cytosolic delivery efficiency to 130%, compared with that in the control condition (Sample 3, 1 h) (Fig. 2A, B). Conversely, no statistically significant improvement was observed under the other conditions. Although the vortex + 0.5 h condition showed a higher mean delivery efficiency (118%, Sample 2) than the control, the vortex + 2 h condition resulted in a lower mean efficiency (91.7%, Sample 6). These

Table 2 Particle size analysis of Pas2r12–EGFP complexes.

Sample No	1	2	3	4	5	6
Vortex mixing	–	+	–	+	–	+
Incubation (h)	0.5	0.5	1	1	2	2
Counts	1738	261	1131	1261	2357	1464
Geo Mean log10 (area μm^2)	0.003	0.000	-0.669	-0.889	0.212	-0.767
Geo Mean (area μm^2)	1.01	1.00	0.214	0.129	1.63	0.171
Diameter (μm)	1.13	1.13	0.52	0.41	1.44	0.47

Pas2r12–enhanced green fluorescent protein (EGFP) complexes were examined using by confocal laser scanning microscopy. In Fig. 3, Geo Mean (log10) values are presented; however, this table summarizes the particle counts, geometric mean, and estimated diameter for each sample.

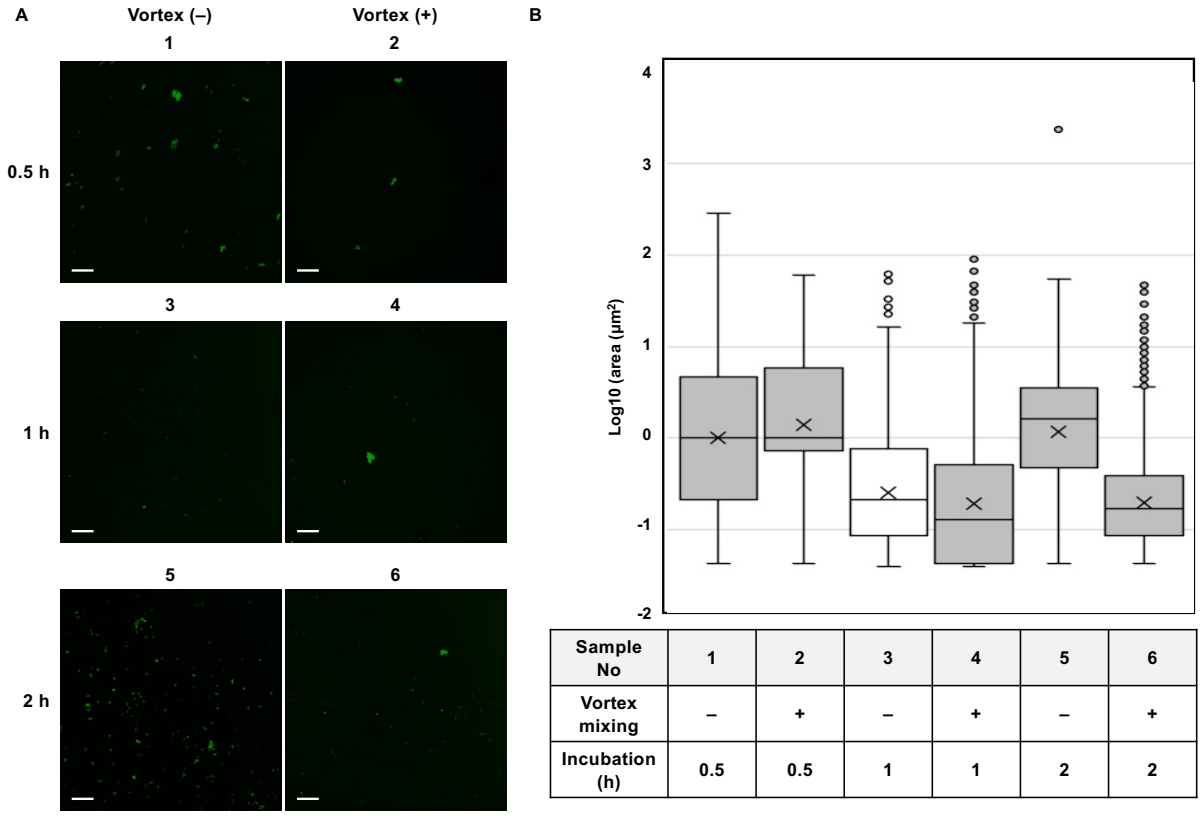

Fig. 3. Visualization and particle analysis of Pas2r12–EGFP complexes by confocal laser scanning microscopy. (A) Confocal laser scanning microscopy images of Pas2r12-enhanced green fluorescent protein (EGFP) complexes. Scale bars represent 20 μm. (B) Particle size distribution is presented on a logarithmic scale.

findings suggest that both the initial mixing process and incubation time influence complex formation and intracellular delivery efficiency.

Pas2r12–EGFP particle size

Particle size analysis by confocal laser microscope revealed marked differences among Samples 1–6. The particle counts were 1,738 (Sample 1: 0.5 h), 261 (Sample 2: vortex + 0.5 h), 1,131 (Sample 3: 1 h, control), 1,261 (Sample 4: vortex + 1 h), 2,357 (Sample 5: 2 h), and 1,464 (Sample 6: vortex + 2 h). The geometric mean areas were 1.01, 1.00, 0.214, 0.129, 1.63, and 0.171 μm^2, corresponding to the estimated diameters of 1.13, 1.13, 0.52, 0.41, 1.44, and 0.47 μm, respectively (Table 2, Fig. 3 A, B). Sample 4 (vortex + 1 h) exhibited the smallest particle size (~0.41 μm), whereas Samples 1 and 5 (0.5 h and 2 h without vortex) formed relatively large particles (>1 μm). Remarkably, vortex mixing combined with short incubation (0.5–1 h) improved the cytosolic delivery efficiency despite differences in particle size.

Altogether, no clear correlation was detected between particle size and cytosolic delivery efficiency. For instance, although Samples 4 and 6 showed similar diameters (~0.41 vs. ~0.47 μm), Sample 6 demonstrated lower delivery efficiency than the control (Fig. 2A, B). These findings suggest that particle size alone is insufficient to explain cytosolic delivery performance.

To further characterize the complexes, Pas2r12–EGFP particles were examined by flow cytometry. FSC, which reflects particle size, increased in Sample 1 (0.5 h) and Sample 6 (vortex + 2 h), suggesting the presence of larger particles (Fig. 4A). Conversely, no marked differences were observed in SSC, which reflects structural complexity, among the experimental conditions (Fig. 4B). Remarkably, EGFP fluorescence intensity decreased under all vortex-treated conditions (vortex + 0.5, 1, and 2 h) (Fig. 4C). The observed reduction in fluorescence intensity may be attributed to multiple factors, including self-quenching within densely packed complexes, irreversible aggregation, conformational changes, and reduced energy transfer efficiency. Furthermore, a decrease in EGFP content within the complexes may contribute to this effect. Nonetheless, these mechanisms cannot be distinguished based on a single parameter.

Particle counts for Samples 1–6 were 594,515, 339,009, 333,973, 1,155,278, 357,155, and 985,787, respectively (Fig. 4D), and were markedly increased in Sample 1 (0.5 h), Sample 4 (vortex + 1 h), and Sample 6 (vortex + 2 h) compared with those in the control. When normalized to the control (Sample 3), particle counts increased by approximately 1.78-fold (Sample 1), 3.46-fold (Sample 4), and 2.95-fold (Sample 6), indicating a pronounced increase particularly in vortex-treated samples with 1–2 h incubation. In addition, confocal microscopy was performed without filtration and thus detects both large aggregates and smaller particles, whereas flow cytometry involves filtration prior to measurement and preferentially detects particles within a defined size range, potentially excluding larger aggregates. To facilitate comparison between the two analytical methods, particle counts were normalized to the control (Sample 3) and compared side by side. Confocal microscopy showed fold changes of approximately 1.54 (Sample 1), 0.23 (Sample 2), 1.11 (Sample 4), 2.08 (Sample 5), and 1.29 (Sample 6) (Table 2), whereas flow cytometry showed corresponding values of 1.78, 1.02, 3.46, 1.07, and 2.95 (Fig. 4D). Notably, Sample 4 exhibited only a modest increase in confocal analysis but a marked increase in flow cytometry, whereas Sample 5 showed the opposite trend. The apparent discrepancy between the results of confocal microscopy and flow cytometry can be explained by differences in sample preparation and detection principles.

Confocal microscopy detects fluorescent aggregates in a two-dimensional imaging plane, including large clusters, whereas flow cytometry measurements were performed after filtration through a nylon mesh, which removes large aggregates before analysis. Importantly, for Samples 2, 4, and 6, there was no significant change in cytosolic delivery efficiency before and after nylon filtration, indicating that the filtration step does not substantially affect functional delivery (Fig. 4E). Although this

validation was not conducted for Samples 1, 3, and 5, all samples were prepared under comparable physicochemical conditions, differing primarily in mixing and incubation parameters. Overall, these considerations suggest that the filtration step is unlikely to substantially bias the interpretation of cytosolic delivery efficiency across different samples.

Structural characterization, uptake mechanisms, and

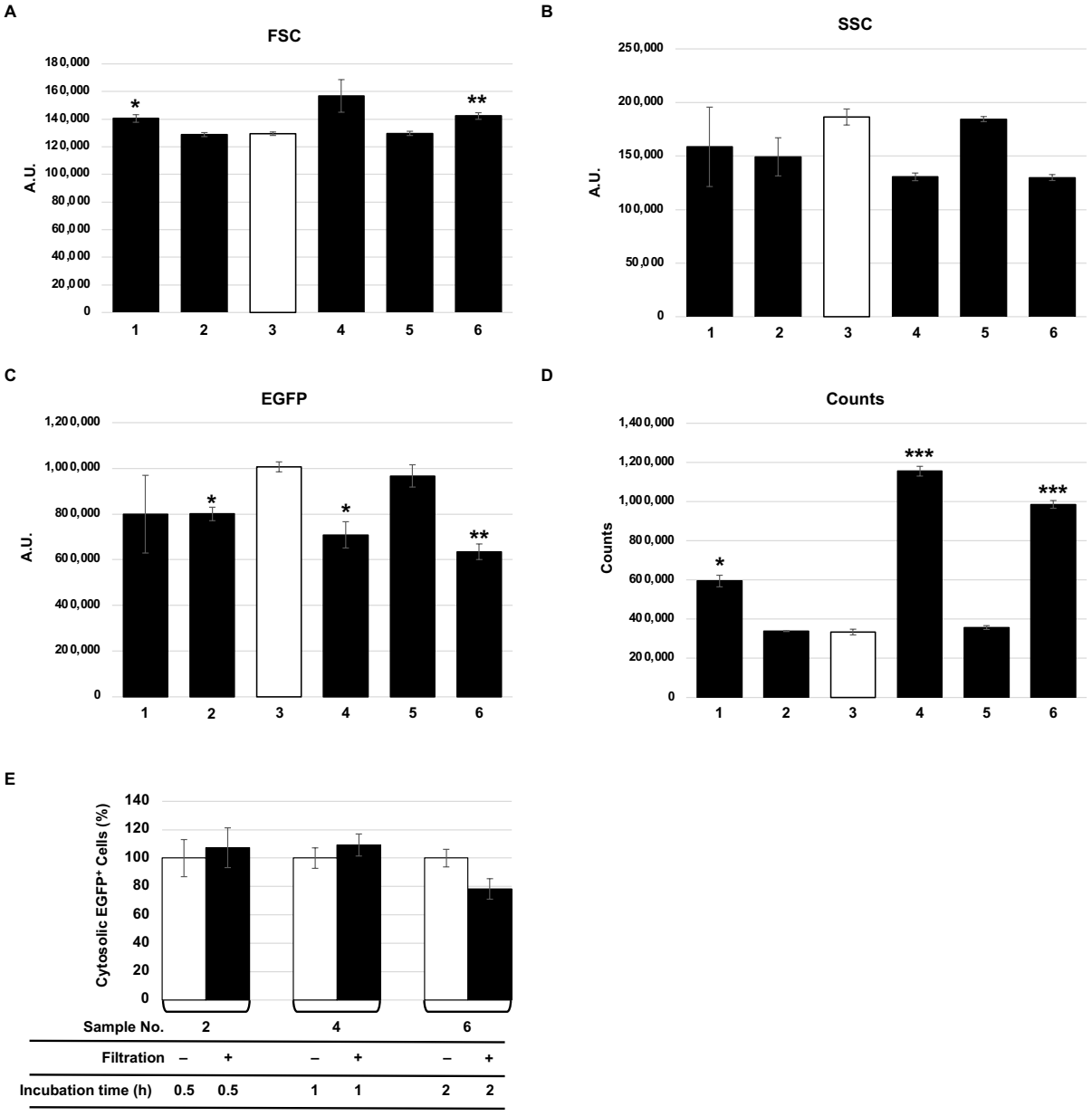

Fig. 4. Analysis of Pas2r12–EGFP complexes by flow cytometry. Forward scatter (FSC, A), side scatter (SSC, B), enhanced green fluorescent protein (EGFP) intensity (C), and particle counts (D) were analyzed. Data were compared with the control condition (Sample 3, 1-h incubation; white column) using one-way analysis of variance (ANOVA) followed by Dunnett's multiple comparison test. Data are expressed as mean ± SD (n = 3). *$p < 0.05$, **$p < 0.01$, ***$p < 0.001$. (E) The cytosolic delivery efficiency of EGFP in HEK293 cells was compared between filtered (+) and unfiltered (–) Pas2r12–EGFP samples (Samples 2, 4, and 6). For each condition, the delivery efficiency of the unfiltered sample was set to 100%, and statistical analysis was conducted using Student's t-test (n = 3).

limitations

An additional factor that may influence complex formation is the mixing procedure prior to incubation. Vortex mixing may enhance the frequency of molecular collisions between Pas2r12 and EGFP, thereby affecting the initial assembly process. Subsequent incubation could further influence the physicochemical properties of the complexes. These sequential processes may contribute to the observed differences in particle size, heterogeneity, and intracellular delivery efficiency.

From the perspective of cellular uptake mechanisms, particle size is a critical determinant. Clathrin-mediated endocytosis (CME) and caveolae-mediated endocytosis (CvME) are generally most efficient for particles in the range of several tens to ~200 nm[20,21]. Caveolae structures are approximately 60–80 nm in diameter[22], which may limit the uptake of larger particles.

In the present study, the observed particle sizes (0.41–1.44 μm) substantially exceeded the typical size range for CME and CvME, suggesting that additional uptake pathways may contribute to efficient internalization. Furthermore, nonselective pathways, such as macropinocytosis, which can accommodate micrometer-sized particles, may therefore also play a role[23]. Although we have previously demonstrated that Pas2r12–EGFP is delivered to the cytosol primarily through caveolae-mediated endocytosis[13], the relatively large particle sizes observed in the present study suggest the coexistence of multiple uptake pathways, with their relative contributions potentially depending on particle size and heterogeneity.

Altogether, these findings suggest that particle size alone is insufficient to explain cytosolic delivery efficiency and that additional physicochemical properties, including particle heterogeneity and structural organization, may also influence intracellular delivery behavior. One limitation of the present study is that the molecular organization and stoichiometric composition of Pas2r12–EGFP complexes were not directly evaluated. Dual fluorescent labeling of Pas2r12 and EGFP may enable simultaneous visualization of each component and facilitate estimation of their relative distribution within the complexes. Furthermore, detailed structural analyses using superresolution microscopy and electron microscopy may provide additional insights into particle architecture and molecular organization[24]. In addition, the present study is limited to complexes formed between Pas2r12 and EGFP. Because proteins vary widely in size, shape, and surface charge, these properties can strongly influence cellular uptake and intracellular trafficking. Therefore, it remains unclear whether the present findings can be generalized to other proteins. Systematic studies using a broader range of protein cargos will be required to establish the general applicability of Pas2r12-mediated intracellular delivery.

Acknowledgments

We would like to thank Enago (www.enago.jp) for the English language editing. This study was supported by JSPS KAKENHI [Grant Numbers 24K08630].

Conflicts of interest

The authors declare no conflict of interest.

References

1. Rizzuti M, Nizzardo M, Zanetta C, Ramirez A, and Corti S: Therapeutic applications of the cell-penetrating HIV-1 Tat peptide. Drug Discov Today, 20:76-85, 2015.
2. Futaki S: Oligoarginine vectors for intracellular delivery: design and cellular-uptake mechanisms. Biopolymers, 84:241-249, 2006.
3. Heitz F, Morris MC, and Divita G: Twenty years of cell-penetrating peptides: from molecular mechanisms to therapeutics. Br J Pharmacol, 157:195-206, 2009.
4. Duchardt F, Fotin-Mleczek M, Schwarz H, Fischer R, and Brock R: A comprehensive model for the cellular uptake of cationic cell-penetrating peptides. Traffic, 8:848-866, 2007.
5. Van Ommen JR, Valverde JP, and Pfeffer R:

Fluidization of nanopowders: a review. J Nanopart Res, 14:737, 2012.
6. Bryła A, Juzwa W, Weiss M, and Lewandowicz G: Lipid nanoparticles assessment by flow cytometry. Int J Pharm, 520:149-157, 2017.
7. Garcia Romeu H, Deville S, and Salvati A: Time- and space-resolved flow-cytometry of cell organelles to quantify nanoparticle uptake and intracellular trafficking by cells. Small, 17:e2100887, 2021.
8. Sikora A, Shard AG, and Minelli C: Size and ζ-potential measurement of silica nanoparticles in serum using tunable resistive pulse sensing. Langmuir, 32:2216-2224, 2016.
9. Filipe V, Hawe A, and Jiskoot W: Critical evaluation of nanoparticle tracking analysis (NTA) by NanoSight for the measurement of nanoparticles and protein aggregates. Pharm Res, 27:796-810, 2010.
10. Shiraishi T, and Nielsen PE: Enhanced delivery of cell-penetrating peptide-peptide nucleic acid conjugates by endosomal disruption. Nat Protoc, 1:633-636, 2006.
11. Takayama K, Nakase I, Michiue H, Takeuchi T, Tomizawa K, Matsui H, and Futaki S: Enhanced intracellular delivery using arginine-rich peptides by the addition of penetration accelerating sequences (Pas). J Control Release, 138:128-133, 2009.
12. Takayama K, Hirose H, Tanaka G, Pujals S, Katayama S, Nakase I, and Futaki S: Effect of the attachment of a penetration accelerating sequence and the influence of hydrophobicity on octaarginine-mediated intracellular delivery. Mol Pharm, 9:1222-1223, 2012.
13. Okuda A, Tahara S, Hirose H, Takeuchi T, Nakase I, Ono A, Takehashi M, Tanaka S, and Futaki S: Oligoarginine-bearing tandem repeat penetration-accelerating sequence delivers protein to cytosol via caveolae-mediated endocytosis. Biomacromolecules, 20:1849-1859, 2019.
14. Okuda A, Kumakura M, Shimizu H, Suto R, and Sugai K: Extracellular signal-regulated kinase 1/2 activation by modified cell-penetrating peptide [Jpn]. Int J Anal Bio-Sci, 46:242-250, 2023.
15. Okuda A, Takihara H, Kuroiwa R, and Okuda S: Phosphoproteomic analysis of signal transduction dynamics induced by a modified cell-penetrating peptide-protein complex. Biochem Biophys Res Commun, 778:152356, 2025.
16. Sugai K, and Okuda A: Role of the Insulin Receptor in Mediating Cytosolic Delivery of Proteins by a Modified Cell-Penetrating Peptide. Pharmaceuticals, 18:1885, 2025.
17. Futaki S, Niwa M, Nakase I, Tadokoro A, Zhang Y, Nagaoka M, Wakako N, and Sugiura Y: Arginine carrier peptide bearing Ni(II) chelator to promote cellular uptake of histidine-tagged proteins. Bioconjug Chem, 15:475-481, 2004.
18. Okuda A and Oikawa A: Effect of fetal bovine serum on the cytosolic protein delivery using modified cell-penetrating peptide [Jpn]. Int J Anal Bio-Sci, 43:314-320, 2020.
19. Schneider CA, Rasband WS, and Eliceiri KW: NIH image to ImageJ: 25 years of image analysis. Nat Methods, 9:671-675, 2012.
20. Conner SD and Schmid SL: Regulated portals of entry into the cell. Nature, 422:37-44, 2003.
21. Rejman J, Oberle V, Zuhorn IS, and Hoekstra D: Size-dependent internalization of particles via the pathways of clathrin- and caveolae-mediated endocytosis. Biochem J, 377:159-169, 2004.
22. Wang Z, Tiruppathi C, Minshall RD, and Malik AB: Size and dynamics of caveolae studied using nanoparticles in living endothelial cells. ACS Nano, 3:4110-4116, 2009.
23. Swanson JA and Watts C: Macropinocytosis. Trends Cell Biol, 5:424-428, 1995.
24. Hell SW: Far-field optical nanoscopy. Science, 316:1153-1158, 2007.